

# 862. Optimal design and experimental verification of a spherical-wheel composite robot with automatic transformation system

Kang Hou<sup>1</sup>, Hanxu Sun<sup>2</sup>, Qingxuan Jia<sup>3</sup>

Department of Automation, Beijing University of Posts and Telecommunications, 100876, Beijing, China

E-mail: <sup>1</sup>houkang87@hotmail.com, <sup>2</sup>hxsun@bupt.edu.cn, <sup>3</sup>sdjxq@sohu.com

(Received 2 July 2012; accepted 4 September 2012)

**Abstract.** This paper presents a design for a dual-mode prototype robot with the advantages of both a spherical robot and wheeled robot. A spherical robot has flexible movement capabilities, and the spherical shell can protect the mechanism and electronic devices. A wheeled mobile robot operates at high speed on a flat road. Its simple structure and control system has made it a popular choice in the field of robotics. Our objective was to develop a new concept robot capable of combining two different locomotion mechanisms to increase the locomotion stability and efficiency. The proposed mobile robot prototype was found to be capable and suitable in different situations. The exchange of modes between the spherical and the wheeled robot was realized by a structural change of the robot. The spherical-wheel mobile robot prototype is composed of a deformable spherical shell system, the propulsion system for the sphere and a wheeled mobile unit module. The exchange of locomotion modes was implemented by changing the geometric structure of spherical shell. The mechanical structure of the composite robot is presented in detail as well as the control system including hardware components and the software. The control system allowed for the automatic transformation of the composite robot between either of the locomotion modes. Based on analysis and simulation, the mechanism was optimized in its configuration and dimension to guarantee that robot had a compact structure and high efficiency. Finally, the experimental results of the transformation and motion processes provided dynamic motion parameters and verified the feasibility of the robot prototype.

**Keywords:** spherical-wheel robot, dual-mode locomotion, simulation and optimization, prototype experiment.

## Introduction

With the continuous development of robotics technology, robots operate in an increasing number of different environments. As a result, the mobility of robots is coming to the attention of scholars all over the world. The multi-modal locomotion robot, which combines two or more kinds of robots in one body, has many locomotion modes to face different environments. Given the conditions of different application environments and tasks, this kind of robot can choose the optimal movement mode and deform itself to move in a stable and reliable manner. Multi-modal locomotion robots have been under extensive research and development in recent years. NASA Jet Propulsion Laboratory (JPL) developed a robot named Go-For, and this robot has wheels at the end of its legs [1]. This wheel-leg composite robot combined the high adaptability of the leg robot and high speed and efficiency characteristics of the wheeled robot. Automation Technology Laboratory in Helsinki University of Technology designed a new platform with hybrid locomotion capability. It is used mainly in an outdoor environment when doing work interactively with a human operator. The purpose of the hybrid platform locomotion system was to provide a rough terrain capability and a wide speed range for the machine at the same time [2]. AZIMUT in IntRoLab is a modular mobile robotic platform that addresses the challenge of making multiple mechanisms available for locomotion on the same robotic platform. AZIMUT has four independent articulations that can be wheels, legs or tracks or a combination of these

[3]. A transformable wheel-track robot with a self-adaptive mobile mechanism, called NEZA-I has been developed at the Chinese Academy of Sciences. It has the merits of both a wheel mechanism and a track mechanism to adapt to the complex and unpredictable environment, where the ground is alternately soft and hard [4]. The authors and their laboratory have investigated the spherical robot for many years [5-7] and developed a variety of spherical, mobile robot prototypes. Based on the spherical robots above, a new kind of robot combining the spherical robot and wheeled robot is designed and optimized to improve reliability and adaptability.

Spherical robots are mobile robots which have the shape of a ball and consist of a drive mechanism and control system inside a spherical shell. It relies on a mechanism for propulsion that effectively relocates the center of gravity of the robot. It has been found that a spherical robot has flexible movement, capabilities and can protect the mechanism and electronic devices in the spherical shell [8-10].

Wheeled mobile robots have been researched and developed for many years [11-13]. These robots can run on the flat road with high speed, and their simple structure and control system has made it a popular choice in the field of robotics. But when this kind of robot has been operated on uneven or soft ground, it faced difficulty in moving because of little surface friction. Therefore, for a wheeled robot the requirement for smooth and hard surface conditions is necessary.

This paper presents design of a composite mobile robot prototype with dual-mode locomotion encompassing rolling mode and wheel-driven mode. The prototype mobile robot adapted to a variety of complex terrain environments. Interchange between the spherical robot and the wheeled robot modes is accomplished by automatic modification of robot geometry. The prototype of the spherical-wheel robot is shown in Fig. 1.



**Fig. 1.** Prototype of the spherical-wheel robot

This paper is organized as follows. The first section provides a description of the composite robot mechanical structure and its characteristics outlining its locomotion capabilities. The second section presents a description of its control system, which includes both the hardware and software components. Also, the process of the transformation is presented in this section. The third section provides simulations of key components to provide theoretical basis to the enhanced feasibility of the composite robot. Based on the analysis and simulation, the mechanism is optimized in configuration and dimension to guarantee the robot with compact structure and high efficiency. The fourth section reports tests results in the transformation process and motion to elicit dynamic motion parameters and verify the feasibility of the robot.

## **Structure**

The spherical-wheel robot prototype combines functionalities of the spherical and wheeled robots in one body. This robot is composed of the deformable spherical shell system, propulsion system for the sphere and the wheeled mobile unit module.

The deformable spherical shell system, which allows the exchange of the modes between the spherical robot and wheeled robot, is a key part of the robot. It includes the spherical shell and the device that allows for spherical shell deformation. The spherical shell is made of many rectangle-shaped slender elastic wires. The wires deform to allow the transformation of the spherical shell. The elastic spherical shell is capable of bearing the weight of the robot itself in rolling mode. The associated compressive deformation of the wires by gravity is not large and does not affect the steady movement of the robot. Fig. 2 shows the device that allows for spherical shell deformation. The two ends of the wires are fixed in a circle pattern to circular plates. The distance between the circular plates is varied by a tensile motor. And the flat plate, fixed at the bottom of the device for spherical shell deformation, is used to hold many sensors and control devices. When the shell is cylindrical the robot could operate via wheel-drive, as shown in Fig. 2(a) where the state of spherical shell is in tension. When the shell is in a sphere shape, the robot can move by rolling, as shown in Fig. 2(b), where the state of the spherical shell is in contraction.

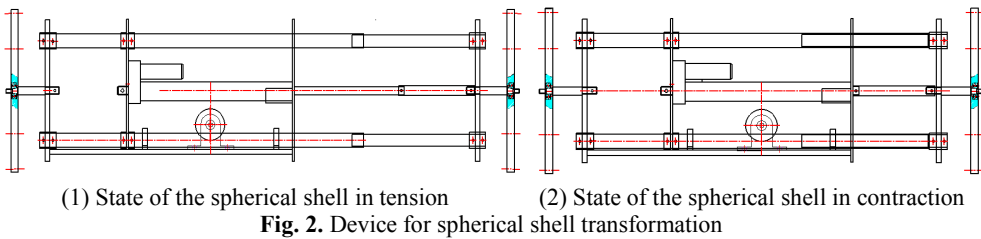
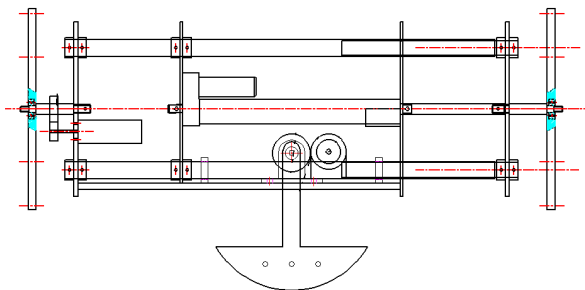


Fig. 3 illustrates the inner propulsion unit that makes the sphere roll when the flexible spherical shell is in the shape of a sphere. It contains a long axis framework, a pendulum and a motor drive system.



In Fig. 3, a long axis motor is fixed on the long axis framework. The long axis motor makes the spherical shell rotate relatively around the long axis framework, and it makes the robot change its center of gravity position. Based on the external friction of the spherical shell, the robot moves forward by rolling. The pendulum is set in the middle of the long axis framework, and the short axis motor makes the pendulum rotate around the short axis. Curvilinear motion of the spherical robot is movement made by changing the angle between the pendulum and the vertical line through the short axis motor. This allows for the omnidirectional movement of the robot.

The four wheel drive system allows the robot to move in a specialized way. The four wheels and the drive motors are installed at the bottom of the long axis platform plate. The wheel control board and drive board are placed on the long axis platform board. The four wheel drive system allows the robot to make a turn with no turning radius and move flexibly. When the

elastic spherical shell is stretched and appears to be cylindrical, the wheels are exposed from the shell through the gaps between the elastic wires and make contact with the ground. Thus, the robot is able to move by four wheel drive.

The robot possesses high environmental adaptability and could accomplish unpredictable tasks through modification of its configuration according to the environment changes and mission requirements: (1) The robot is able to move with four-wheel drive when it is operated on the flat road with high speed and robustness; (2) When it is operated on uneven or soft surface, it is very difficult to move by wheel propulsion, but the robot is able to move steadily and rapidly by transforming into a sphere and rolling; (3) When it tried to pass a narrow area, the robot can adapt to four-wheel drive in order to shorten the horizontal length of the composite robot; (4) If the wheels of the robot are stuck in the mud or get damaged, it can go on moving by changing from the wheel-drive to spherical rolling mode.

### Control system

**1) Hardware.** The control system contains many components. There is a central controller board, the motor driven devices, tensile motor, sensors, power supply and a voltage conversion board. The composite spherical-wheel robot hardware is placed inside the long axis framework of the robot. The diagram of the composite robot hardware is presented in Fig. 4.

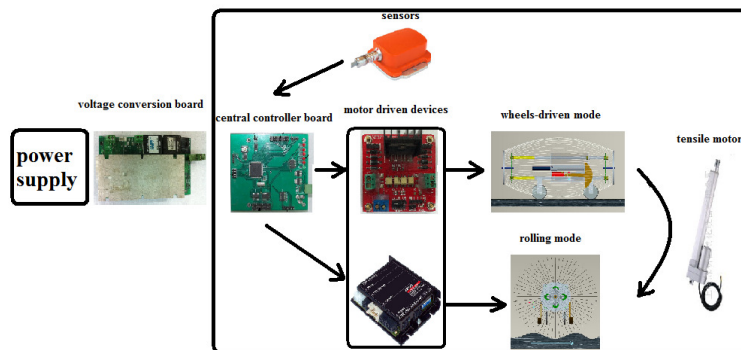
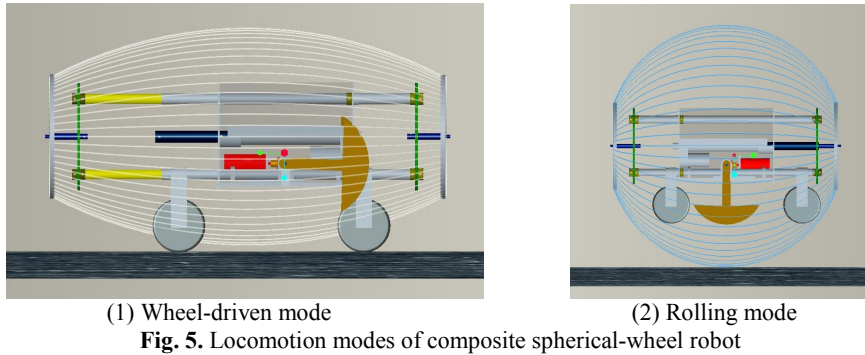


Fig. 4. Hardware of the composite robot

The power supply is connected to the voltage conversion board to provide constant voltages for the central controller board which operates on 5 Volts, motor-driven devices requiring 24 Volts and the sensors powered by 12 Volts. The central controller board contains a CAN bus interface and RS-232 serial interface, and connects all the sensors and motor driven devices to receive and send the commands. This board was designed with all possible variations and expansion capabilities (such as I/O interfaces) for other applications. It has status indicator lights to indicate instruction execution stages. There are two motor driven devices for the rolling mode, a long axis motor and a short axis motor, and four motor driven devices for the four-wheel drive system. They connect the central controller board with the CAN bus interface and I/O interfaces respectively. The tensile motor contains the drive system inside so it connects to the central controller board directly by the I/O interface. The sensors, which include the gyroscope, the GPS system and other extension devices, communicate with the main controller board by the RS-232 serial interface.

**2) Software.** In the central controller board, the software was developed for the overall control of the composite spherical-wheel robot. It follows a general procedure that allows it to examine all devices, to complete a self-diagnostic test, to receive the data from its sensors, and to give commands to the driven systems of the actuators. The process of robot automatic

transformation is provided as follows. The locomotion modes of the composite spherical-wheel robot are shown in Fig. 5.



In order to change the shape of the robot into a sphere (Fig. 5(1) goes to Fig. 5(2)), the programmed procedure has two steps. Firstly, the spherical shell is contracted into the shape of a sphere by the tensile motor. This results in four wheels then being located inside the spherical shell. In the second step the pendulum is then set from the level position of the long axis to the vertical position by the short axis motor. The robot is then capable of transforming by means of the coordinated movement of the long axis motor and the short axis motor.

The procedure to allow for wheeled movement (Fig. 5(2) goes to Fig. 5(1)) is just the opposite. In the first step the short axis motor turns the pendulum to the level position of the long axis framework. In the second step the spherical shell is stretched by the tensile motor to make it a cylindrical or similar to a cylindrical. Then the wheels are exposed from the spherical shell through the gaps between wires and make contact with the ground to move ahead.

### Analysis and simulation

During the design of the robot, it was found that the spherical shell was the most important part of the robot transformation to analyze. The spherical shell determines the size of many parts such as wheels and tensile motor. So the analysis and simulation of the spherical shell was undertaken to establish several important mechanical design parameters. From those results, the size and parameters of wheels and tensile motor were modeled and optimized. The mechanism was optimized in configuration and dimension in order to guarantee the robot has a reasonable structure, effective motion and high efficiency.

**1) Spherical shell analysis.** The spherical shell, as the key part of the composite robot, is constructed of a number of elastic wires. These wires allow for the exchange between the spherical robot and wheel robot by bending and straightening. Through the analysis of the wires, we obtained ranges of mechanical design parameters in the transformation process. These design parameters were necessary in order to design other parts of the robot. The diagram of the spherical shell wire is shown in Fig. 6. The parameters of an elastic wire are shown in Fig. 6 and listed in Table 1.

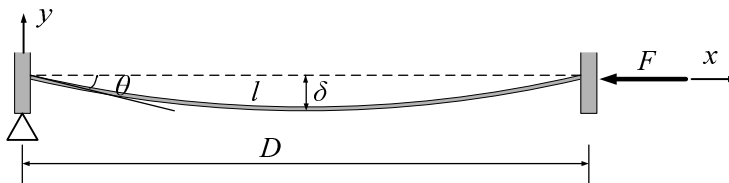


**Fig. 6.** Single wire of the spherical shell modeled as a slender column

**Table 1.** Parameters of elastic wire

Description	Parameters
Length of wire	$l$
Horizontal distance between the ends of wire	$D$
Vertical displacement of wire along $y$ -axis	$\delta$
Angle between the wire and $x$ -axis	$\theta$
Wire arc length	$s$
Force along $x$ -axis	$F$

The wire of the spherical shell was modeled as a pin-ended slender column with these two assumptions. The length of wire was much larger than the radius of the cross-section. Also the movement of the elastic wire was limited only by the axial force [14].

From Fig. 6, we can get an analytical representation of the elastic curve as:

$$EI \frac{d\theta}{ds} + Fy = 0 \tag{1}$$

where  $E$  denotes elastic modulus of the wire, and  $I$  denotes cross-sectional area moment of inertia.

Based on Eq. (1), after the process of integration and completing the differential, one finds that force along  $x$ -axis is:

$$F = \left[ \frac{2}{\pi} K \left( k, \frac{\pi}{2} \right) \right]^2 F_0 \tag{2}$$

Vertical displacement of wire along  $y$ -axis:

$$\delta = \frac{k}{K \left( k, \frac{\pi}{2} \right)} l \tag{3}$$

Horizontal distance between the ends of wire:

$$D = \left[ 2 \frac{E \left( k, \frac{\pi}{2} \right)}{K \left( k, \frac{\pi}{2} \right)} - 1 \right] l \tag{4}$$

where  $k = \sin \theta/2$ ,  $K \left( k, \frac{\pi}{2} \right)$  is the complete elliptic integral of the first kind,  $E \left( k, \frac{\pi}{2} \right)$  is the

complete elliptic integral of the second kind and  $F_0 = \frac{\pi^2 EI}{l^2}$  is a critical load for pin-ended column.

**2) Deformation of spherical shell under gravity.** The spherical shell is affected by the force of gravity on the robot, and the parts of the shell which have contact with the ground deform in shape. The magnitude of deformation is determined by robot weight, elastic properties and cross-sectional area of the wires. Fig. 7 shows the schematic diagram of wire deformation under gravity.

The following derivation was performed to obtain analytical relationship for the deformation of the wires under the force of gravity. The total energy of wire deformation can be written as [15-17]:

$$W = \frac{4P}{R^2} (1 + \mu) S_i + \frac{2\pi a^{1/2} E h^{5/2} \alpha^{5/2}}{12^{3/4} (1 - \mu)} J_0 - \frac{4(1 - \mu) \alpha \pi a P}{R} \tag{5}$$

where  $J_0 \approx 1.15$ ,  $P$  is the flexural rigidity of wire,  $S_i = \pi aw$ ,  $w$  is wire width, and  $\mu$  is Poisson's ratio.

$$W = 2\pi CE(2d)^{3/2} h^{5/2} (1/R) \tag{6}$$

where  $C = J_0/[12^{3/4}(1-\mu^2)]$ .

$$W = T_G \tag{7}$$

where  $T_G = Md$ , and  $M$  is the mass of the robot.

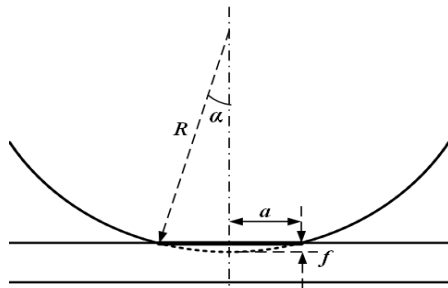


Fig. 7. Schematic diagram of wire deforming under gravity

Then one finds that:

$$d = \sqrt{\frac{M^2 R^2}{(2h)^5 \pi^2 C^2 E^2}} \tag{8}$$

FEM simulation software was used to analyze the deformation of the elastic wires. ANSYS 11.0 Mechanical Work Environment was employed to simulate elastic deformation of the wires. The results of simulation of the robot prototype under the force of gravity are provided in Fig. 8.

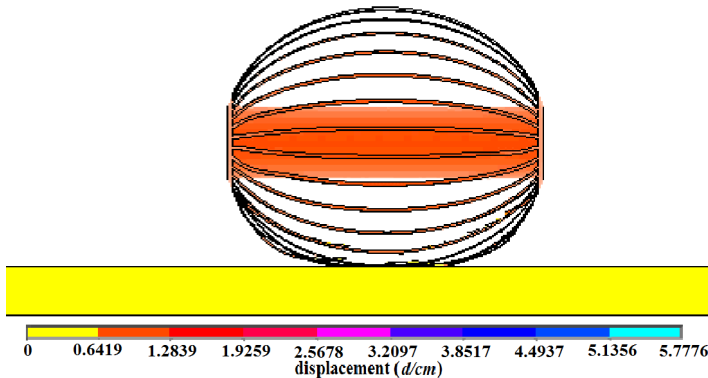


Fig. 8. Simulation diagram depicting robot displacement under gravity

Simulation results obviously reveal that spherical shell deformation under the influence of gravity of the robot is significant. In practical tests, it was determined that elastic wires of circular cross-section are distorted more under the force of gravity than ones of rectangular cross-section. Thus, rectangle-shaped elastic wires were chosen to make the spherical shell in the simulation and in the actual prototype. In the above simulation, it was determined that the robot, under the force of gravity, has more than one elastic wire in contact with the ground in comparison to the state of a spherical shape. This is consistent with observations in the actual prototype.

**3) Wheel analysis.** In the wheeled robot mode, the wheels have to reach the ground through the gap of the neighboring wires. So the width of the wheel  $d_w$  needs to satisfy the objective function:

$$d_w < d_G \tag{9}$$

where  $d_G$  is the width of the gap between the neighboring wires for wheels.

As shown in Fig. 9,  $H_L$  is the height of the long axis. So measured from the middle of wire diameter  $D_M$ :

$$D_M = H_L + 2\delta \tag{10}$$

The number of wires was set at 20, so the maximum distance between the neighboring wires can be computed from:

$$d_{nw} = \frac{\pi D_M}{20} \tag{11}$$

The wheels are attached at a location that is one quarter of the length of the long axis. So the analysis is simplified, and the gap width between the neighboring wires is equal to half of the maximum distance between the neighboring wires:

$$d_G = \frac{1}{2} \frac{\pi D_M}{20} \tag{12}$$

Given that the spherical shell elastic material length  $l = 80$  cm, from Eq. (3), then  $\delta = 3.6$  cm. Also from Eq. (10),  $D_M = 23 + 2 \times 3.6 = 30.2$  cm, and from Eq. (11),  $d_{nw} = 4.74$  cm. So the result satisfies the function  $d_w < d_G = 2.37$  cm.

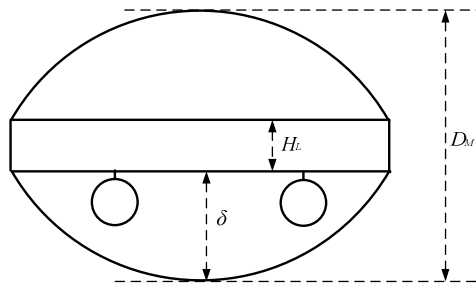
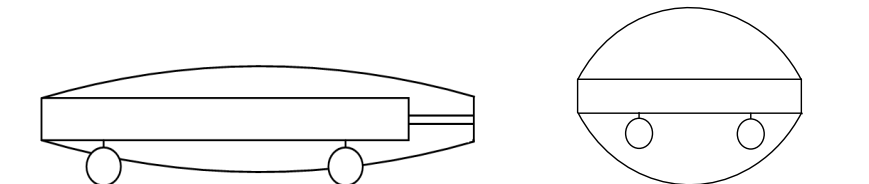


Fig. 9. Schematic diagram for wheels

For the two modes of the prototype robot, the wheel robot mode and the spherical robot mode, we found an optimal range for the size of the wheel radius. The principles that were used to design the wheel size are explained here and shown schematically in Fig. 10. When the robot is in a wheeled mode, the lowest point of the spherical shell is required to be higher than the lowest point of the wheel. From the application of this principle, shown in Fig. 10(a), the minimum value of the wheel radius is derived. Another principle is that when the robot is in a spherical mode, the lowest point of the wheel must be higher than the lowest point of the spherical shell. From the application of this principle, shown in Fig. 10(b), the maximum value of the wheel radius is obtained.



(a) Wheeled robot mode

(b) Spherical robot mode

Fig. 10. Schematic diagram of composite prototype robot in two different modes

In Fig. 10(a), the wheel radius  $\rho$  needs to satisfy the requirement for  $\rho > \delta_{\min}$ , where  $\delta_{\min}$  is the value of  $\delta$  in the wheeled robot mode. In Fig. 10(b), in order not to affect the spherical robot performance while undergoing turning movement, the wheels needed to be inside the spherical shell. So from these conditions, a relationship was formed among the variables such that the wheel radius satisfies  $\rho < \frac{1}{2}\delta_{\max}$ , where  $\delta_{\max}$  is the value of  $\delta$  in the spherical robot mode. So the design of the wheel radius needs to satisfy the objective function:

$$\delta_{\min} < \rho < \frac{1}{2}\delta_{\max} \tag{13}$$

Given that the spherical shell elastic material length  $l = 80$  cm, and that, from the horizontal, the different angles  $\theta$  between the wires were  $\theta = 30^\circ$  in wheeled robot mode and  $\theta = 75^\circ$  in spherical robot mode. Then, according to Eq. (3) and (13), the range of wheel radius is  $3.35 \text{ cm} < \rho < 8.43 \text{ cm}$ .

**4) Tensile motor analysis.** A tensile motor was necessary to make the prototype transform between the spherical robot mode and the wheeled robot mode. So the tensile motor allowed for the maximum change of the distance between the ends of wire. The requirement was for the maximum length of the tensile motor extension  $L_T$  should satisfy the objective relationship:

$$L_T > \Delta D_{\max} \tag{14}$$

where  $\Delta D_{\max}$  is the maximum change of horizontal distance of the ends of wire  $D$  between the spherical robot mode and the wheeled robot mode.

In Fig. 10, the angle  $\theta = 30^\circ \sim 75^\circ$  was established. Also, from Eq. (4), established were the distance between the ends of wire  $D = 74.59 \text{ cm} \sim 48.64 \text{ cm}$ ,  $\Delta D_{\max} = 25.95 \text{ cm}$ , and the max length of tensile motor extension  $L_T > \Delta D_{\max} \approx 26 \text{ cm}$ .

## Experiments

Based on the above structural design and analysis of the deformable robot, a spherical-wheel mobile robot prototype was developed. The chassis of the robot prototype was made of aluminum and steel parts. Special-shaped wires made of 65# managanese steel were chosen for the spherical shell because of their high flexibility. Key specifications of the composite spherical-wheel robot are listed in Table 2.

**Table 2.** Specifications of the spherical-wheel robot prototype

Description	Value
Length of elastic wires (cm)	80
Number of elastic wires	20
Cross-section area of elastic wires (cm <sup>2</sup> )	0.7×0.25
Frame size of long axis (length×width×height) (cm×cm×cm)	70×20×20
Diameter of circular plate (cm)	23
Wheel radius (cm)	6.25
Width of wheel (cm)	2
Max length of tensile motor's extension (cm)	30
Total mass (kg)	14.7

The validity of the proposed prototype design was verified with some experimental tests. Experimental tests were carried out in a room. The tests were aimed at validating the robust operation of the prototype in several environmental and operational conditions. Those environmental and operational conditions include 1) motions when the prototype is required to transform from one type of locomotion to another, 2) forward motion under spherical locomotion, and 3) climbing of a stair under spherical locomotion. In particular, some

parameters were measured to characterize the performance such as the amount of deformation of the shell wires, velocity of spherical movement and performance overcoming obstacles.

**1) Deformation test.** The deformation test evaluated the performance of the transforming system. A simulation based on Eq. (3) and (4) was compared with experimental results. During the process of transformation, there comes a time when the wheels touch the ground. Since it was hard in the experiment to actually measure the deformation, in this instance the deformation was assigned a value of zero. But when the spherical shell touches the ground, we actually measured the vertical distance between the end of wire and the point contacted with the ground rather than the deformation directly. Fig. 11 shows the results of experiment and simulation for the shell deformation. In Fig. 11, x-axis represents the horizontal distance between the ends of wire  $D$ , and y-axis represents the vertical distance between the end of wire and the point that makes contact with the ground. In a comparison of the two results, it was found that they are largely consistent. Moreover, when the distance between the ends of wire  $D$  is greater than 72.5 cm, then the experimental result of vertical distance between the end of wire and the point that makes contact with ground  $\delta$  is less than the analytical result mainly due to the effect of the force of gravity on the robot. When  $D$  is less than 72.5 cm, the experimental result is closer to the analytical result because the deformation of spherical shell was rarely affected by gravity in the spherical mode.

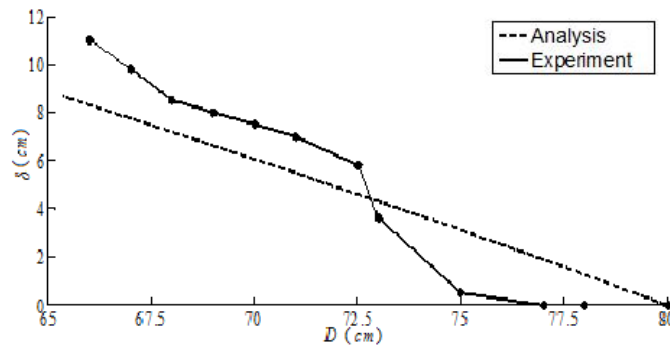


Fig. 11. Deformation of a spherical shell

**2) Velocity test of spherical mode.** Some experiments were performed with the composite robot prototype in spherical mode to test its mobility and stability while operating on the flat ground and moving linearly. The robot velocity was set at 0.3 m/s, and Sensor Dynamics W6DoF was used as the sensor to measure the acceleration of the robot. The speed values were obtained by integrating the values derived from the sensor. Fig. 12 provides experimental results for the velocity of the spherical mode operation. In Fig. 12, x-axis represents the time and the y-axis represents the velocity of the robot forward movement. These results indicate that the velocity of the robot fluctuates because of the spherical shell. Robot moves forward with great fluctuations in speed because of the gaps between the wires and elastic deformation of the wires. In the figure the leading edge of the peak, the time in between the minimum and maximum of the functional curve, physically represents the process of rolling across a wire. Compared to the wheeled-mode movement, the stability of the spherical mode motion is lower.

**3) Motion test of spherical mode climbing up a stair.** Robots usually face many obstacles such as bumpy roads or stairs. Therefore, the capability of a robot prototype to be able to climb was a basic requirement of this composite robot. The robot cannot deal with an obstacle like a stair by using the wheel mode due to the operational limitations of the wheels. But it can change body shape from the wheel mode to the spherical mode to climb up the stairs. Fig. 13 shows the process of the robot prototype climbing on a stair.

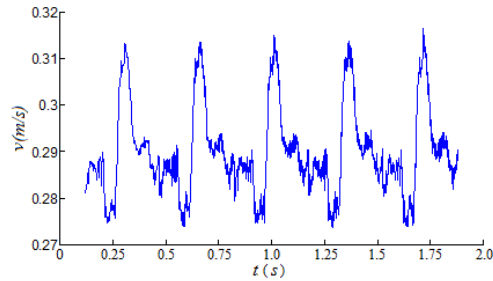


Fig. 12. Velocity of spherical pattern on flat ground

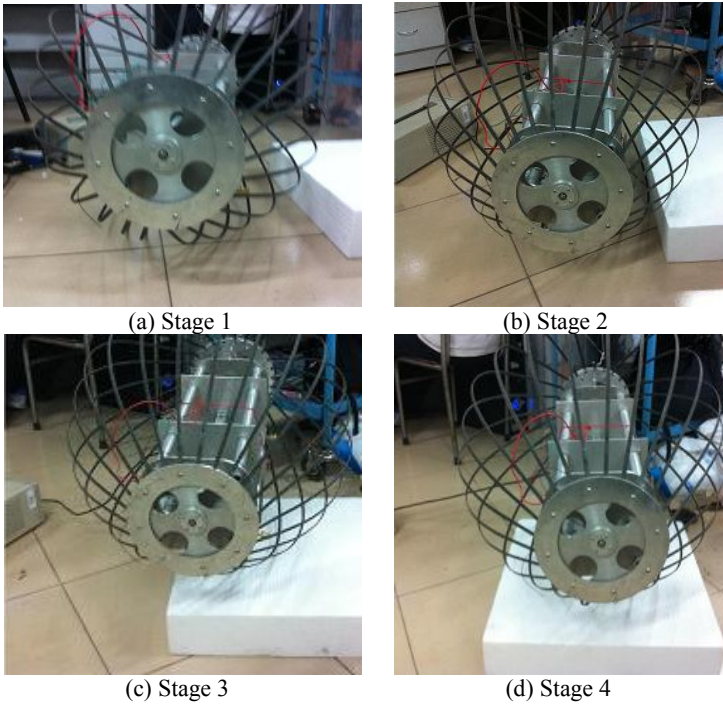


Fig. 13. Stages of robot prototype climbing on a stair

For this test, the obstacle was a white cube obstacle with a height of 10 cm. There were four stages to accomplish the process of climbing the obstacle. In Stage 1, the robot approached the obstacle with a certain speed in spherical mode; in Stage 2, the robot moved close to the obstacle, and one wire contacted the top face of the stair; in Stage 3, the wire on top of the stair acted as a fulcrum, and with the assistance of a heavy pendulum, lifted robot body on top of the stair; in Stage 4, the robot moved forward on the stair. In this test, the robot demonstrated good performance climbing over the stair.

## Conclusions

In this paper, we presented a composite spherical-wheel mobile robot prototype. A spherical-wheel robot is a kind of mobile robot that can move in a variety of complex terrain environments based on its unique combination of the spherical and wheeled modes of locomotion. The methods and means of designing the structure, control system and software of the robot were presented. Based on the geographical location, the robot compares the

characteristics of the spherical and wheeled modes of locomotion and selects the best movement mode to maintain the efficiency and stability. Key parameters of the composite robot were analyzed for determination of the effective structure. A physical prototype based on the above design was introduced and experimentally tested. The experimental results of the transformation and motion processes provided motion parameters and verified the feasibility of the robot. At the same time, its effective dual-mode structure provided the robot with a redundant mechanism, which promotes the robustness of the robotic system. Therefore, the robot could be widely applied in the future.

### Acknowledgements

This research is supported financially by the National Natural Science Foundation of China (No. 50775013), and the Cultivation Fund of the Key Scientific and Technical Innovation Project, Ministry of Education of China (No. 708011).

### References

- [1] **Sreenivasan S. V., Wilcox B. H.** Stability and traction control of an actively actuated micro-rover. *Journal of Robotic Systems*, Vol. 11, Issue 6, 1994, p. 487 – 502.
- [2] **Halme A., Leppanen I., Suomela J.** Workpartner: interactive human-like service robot for outdoor applications. *The International Journal of Robotics Research*, Vol. 22, Issue 7, 2003, p. 627 – 640.
- [3] **Michaud F., Letourneau D.** Multi-modal locomotion robotic platform using leg-track-wheel articulations. *Autonomous Robots*, Vol. 18, 2005, p. 137 – 156.
- [4] **Li Z. Q., Ma S. G., Li B., Wang M. H., Wang Y. C.** Development of a transformable wheel-track robot with self-adaptive ability. *Chinese Journal of Mechanical Engineering*, Vol. 47, Issue 5, 2011, p. 1 – 10.
- [5] **Sun H. X., Xiao A. P., Jia Q. X.** Omnidirectional kinematics analysis on bi-driver spherical robot. *Journal of Beijing University of Aeronautics and Astronautics*, Vol. 31, Issue 7, 2005, p. 735 – 739.
- [6] **Hou K., Sun H. X., Jia Q. X.** An autonomous positioning and navigation system for spherical mobile robot. *Procedia Engineering*, Vol. 29, 2012, p. 2556 – 2561.
- [7] **Liu D. L., Sun H. X., Jia Q. X.** Nonlinear sliding-mode motion control of a spherical robot. *Robot*, Vol. 30, Issue 6, 2008, p. 498 – 502.
- [8] **Kim J., Kwon H., Lee J.** A rolling robot: design and implementation. *Proceedings of the 7<sup>th</sup> Asian Control Conference*, Hong Kong, China, August 27-29, 2009, p. 1474 – 1479.
- [9] **Yue M., Liu B. Y.** Design of adaptive sliding mode control for spherical robot based on MR fluid actuator. *Journal of Vibroengineering*, Vol. 14, Issue 1, 2012, p. 196 – 204.
- [10] **Cai Y., Zhan Q., Xi X.** Neural network control for the linear motion of a spherical mobile robot. *International Journal of Advanced Robotic Systems*, Vol. 8, Issue 4, 2011, p. 79 – 87.
- [11] **Rollins E., Luntz J., Foessel A.** Nomad: a demonstration of the transforming chassis. *IEEE International Conference on Robotics and Automation*, 1999, Leuven, Belgium: IEEE, 1998, p. 679 – 684.
- [12] **Esher T., Cransaz Y., Merminod B.** An innovative space rover with extended climbing abilities. *Proceedings of Space and Robotics*, February 27–March 2, 2000, Albuquerque, USA: ASCE, 2000, p. 781 – 786.
- [13] **Caracciolo L., de Luca A., Iannitti S.** Trajectory tracking control of a four-wheel differentially driven mobile robot. *IEEE International Conference on Robotics and Automation*, 1999, Detroit, USA: IEEE, 1999, p. 2632 – 2638.
- [14] **Timoshenko S. P., Gere J. M.** *Theory of Elastic Stability*. McGraw Hill, New York, 1961.
- [15] **Norman J.** *Structural Impact*. Cambridge University Press, Cambridge, 1989.
- [16] **Gupta N. K., Madhu V.** Normal and oblique impact of a kinetic energy projectile on mild steel plates. *International Journal of Impact Engineering*, Issue 12, 1992, p. 333 – 344.
- [17] **Levg N., Goldsmith W.** Normal impact and perforation of thin plates by hemispherically tipped projectile. *International Journal of Impact Engineering*, Issue 2, 1984, p. 209 – 229.